DECONFINEMENT AND THE EXPLICIT CENTER SYMMETRY BREAKING IN A STRONG MAGNETIC FIELD*

Michał Szymański

Institute of Theoretical Physics, University of Wrocław
50-204 Wrocław, Poland

(Received November 25, 2020)

We show that external magnetic fields increase the strength of explicit center symmetry breaking induced by dynamical quarks. To study the consequences on deconfinement, we perform a schematic mean-field calculation of the Polyakov loop and its fluctuations, and find that the transition is shifted towards lower temperatures. We also show qualitatively how light quarks affect the magnetic field dependence of the deconfinement temperature in an effective model.

DOI:10.5506/APhysPolBSupp.14.415

1. Introduction

Understanding of the impact of strong magnetic fields on deconfinement is important for a proper description of non-central heavy-ion collisions, neutron stars as well as the early Universe [1]. Although gluons are not electrically charged, they couple to the magnetic field indirectly due to the electric charge of quarks. This results in a non-trivial interplay between strong interactions and electromagnetic forces. Particularly, the deconfinement is sensitive to the external magnetic field [2–4].

Deconfinement is mostly understood in the pure gauge theory where it can be related to the spontaneous breaking of the Z_3 center symmetry [5, 6]. The Polyakov loop [7–9], which probes the free energy of a static color source immersed in a hot medium, is a usual choice of the order parameter in this theory. Its expectation value is zero below the critical temperature and the system is invariant under the center symmetry. Above the critical temperature, the Polyakov loop expectation value is finite and the center symmetry is spontaneously broken. For three colors, the transition is first-order.

* Presented at the on-line meeting *Criticality in QCD and the Hadron Resonance Gas*, Wrocław, Poland, July 29–31, 2020.

In the presence of dynamical quarks, the Z_3 symmetry is broken explicitly and for a sufficiently large breaking, deconfinement turns into the second-order transition and then into a crossover. In the last case, the Polyakov loop is no longer a true order parameter but nevertheless it remains a useful probe of the screening properties of the QCD medium [10].

Susceptibilities of the Polyakov loop are another observables relevant for studying deconfinement [11]. They are discontinuous at the first-order transition and have a peak in the case of the crossover which provides a way to define a (non-unique) pseudo-critical temperature. Additional observable sensitive to deconfinement is the ratio of the transverse (imaginary) to longitudinal (real) susceptibilities. In the pure gauge theory, this quantity exhibits a step-function behavior [11, 12]. When light dynamical quarks are included, this ratio becomes considerably smoothened but remains sensitive to deconfinement [12, 13]. It is also useful as it provides means to quantify the strength of explicit center symmetry breaking [14]. Another interesting observable is the static quark entropy, defined as the temperature derivative of the static quark free energy, which was argued to provide a more reliable way to extract the critical temperature of deconfinement than the Polyakov loop inflection point when calculated on the lattice [13].

In this work, we discuss the effect of a strong magnetic field on deconfinement in the heavy-quark limit. To this end, we employ an effective Polyakov loop model in which the effect of quarks is modeled as a linear breaking term coupled to the Polyakov loop. We show that the magnetic field increases the strength of Z_3 symmetry breaking and hence shifts the deconfinement towards lower temperatures. Finally, we discus the case of light quarks within the PNJL model and show how the problem of increasing deconfinement temperature can be understood with our approach.

2. Effective Polyakov loop model

In this work, we model the effective QCD potential as

$$\mathcal{U} = \mathcal{U}_G + \mathcal{U}_Q \,, \tag{1}$$

where $\mathcal{U}_G$ is the pure gauge Polyakov loop potential and $\mathcal{U}_Q$ contains the contribution due to dynamical quarks. The former exhibits the spontaneous center symmetry breaking, while the latter breaks this symmetry explicitly.

To describe the pure gauge sector, we employ the effective potential from Ref. [12]

$$\frac{\mathcal{U}_G}{T^4} = -\frac{A}{2} L\bar{L} + B \ln M_{\mathrm{H}}\left(L, \bar{L}\right) + \frac{C}{2}\left(L^3 + \bar{L}^3\right) + D\left(L\bar{L}\right)^2 , \tag{2}$$

where

$$L = x + iy \,, \qquad \bar{L} = x - iy \tag{3}$$

are the Polyakov loop and its conjugate, and $M_{\rm H}(L,\bar{L})$ is the SU(3) Haar measure

$$M_{\rm H}\left(L,\bar{L}\right)=1-6L\bar{L}+4\left(L^3+\bar{L}^3\right)-3\left(L\bar{L}\right)^2 . \tag{4}$$

Parameters of the potential were obtained using the pure gauge data on the Polyakov loop expectation value and its fluctuations (see Ref. [12] for their exact form).

The effect of dynamical quarks is modeled with the one-loop effective potential

$$\frac{\mathcal{U}_Q}{T^4}=-\frac{2}{T^3}\sum_f\int\frac{{\rm d}^3p}{(2\pi)^3}\left(\ln g_f\left(m,T,L,\bar{L}\right)+\ln g_f\left(m,T,\bar{L},L\right)\right) , \tag{5}$$

where the sum runs over different quark flavors and

$$g_f\left(m,T,L,\bar{L}\right)=1+3L\,{\rm e}^{-\beta E_f}+3\bar{L}\,{\rm e}^{-2\beta E_f}+{\rm e}^{-3\beta E_f} , \tag{6}$$

with $E_f^2=\vec{p}^{\,2}+m_f^2$, where m_f is the mass of the f-flavor quark. For the purpose of studying the Polyakov loop and its fluctuations, this potential can be approximated by the linear form

$$\frac{\mathcal{U}_Q}{T^4}\approx\frac{\mathcal{U}_0}{T^4}-hx+O\left(x^2,y^2\right) , \tag{7}$$

where $\mathcal{U}_0$ is the leading fermion contribution to the pressure, irrelevant for studying the Polyakov loop physics, and

$$h=-\left.\frac{\partial\left(\mathcal{U}_Q/T^4\right)}{\partial x}\right|_{L=0}=\sum_f h_Q\left(m_f,T\right) , \tag{8}$$

with

$$h_Q(m,T)=\frac{12}{T^3}\int\frac{{\rm d}^3p}{(2\pi)^3}\frac{{\rm e}^{-\beta E}+{\rm e}^{-2\beta E}}{1+{\rm e}^{-3\beta E}}\approx\frac{12}{T^3}\int\frac{{\rm d}^3p}{(2\pi)^3}{\rm e}^{-\beta E} , \tag{9}$$

where the second approximation holds in the limit of heavy quarks ($m/T\gg1$) in which only the leading Boltzmann factor contributes in Eq. (9). Then the integral can be calculated analytically

$$h_Q(m,T)\approx\frac{6}{\pi^2}\left(\frac{m}{T}\right)^2K_2\left(\frac{m}{T}\right) , \tag{10}$$

where $K_\nu(x)$ is the modified Bessel function of the second kind. The left panel of Fig. 1 shows the temperature dependence of $h_Q(m,T)$ for quark masses 0.005 GeV (the dashed red line), 0.5 GeV (the dash-dotted blue line) and 1 GeV (the solid black line). The explicit breaking strength tends to a constant for small quark masses and decreases as the quark mass increases.

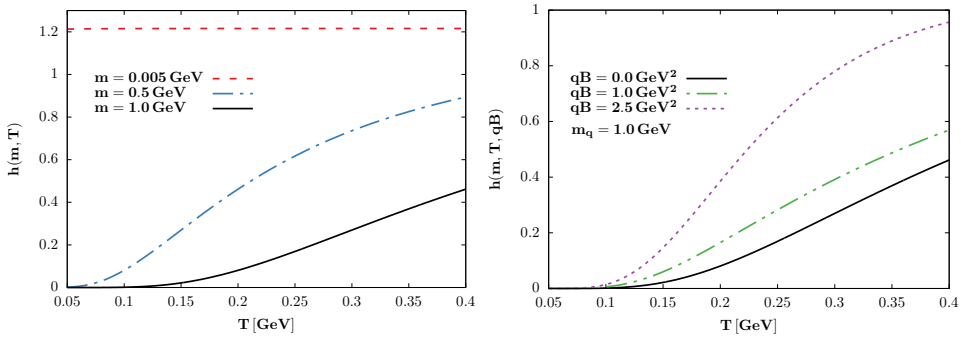

Fig. 1. (Color online) Temperature dependence of the explicit center symmetry breaking strength for different quark masses and vanishing magnetic field (the left panel) and for the fixed quark mass and different magnetic fields (the right panel).

In the presence of a constant and homogeneous magnetic field, quarks undergo Landau quantization and, consequently, their dispersion relation takes the following form:

$$E_{f,k,\sigma}^2 = m_f^2 + p_z^2 + (2k + 1 - \sigma)|q_f B|\,, \tag{11}$$

where the subsequent Landau levels are quantified by $k = \{0, 1, 2 \dots\}$ and $\sigma = \pm 1$. In thermodynamic quantities, the sum over states becomes modified accordingly

$$2 \int \frac{\mathrm{d}^3 p}{(2\pi)^3} \to \frac{|qB|}{2\pi} \sum_{\sigma=\pm 1} \sum_{k=0}^{\infty} \int_{-\infty}^{\infty} \frac{\mathrm{d}p_z}{2\pi}\,, \tag{12}$$

where the summation runs over Landau levels and the factor $|qB|/(2\pi)$ accounts for the planar density of each Landau level. Consequently, the explicit Z_3 breaking term becomes a function of magnetic field

$$h = \sum_f h_Q^B \left(m_f, T, q_f B\right)\,, \tag{13}$$

where $h_Q^B(m, T, qB)$ is obtained by applying prescription (12) into Eq. (9). In the heavy-quark approximation, it can be written as

$$h_Q^B(m, T, qB) = \frac{3|qB|}{\pi^2 T^3} \sum_{\sigma=\pm 1} \sum_{k=0}^{\infty} M_{k,\sigma} K_1 \left(\frac{M_{k,\sigma}}{T}\right)\,, \tag{14}$$

where

$$M_{k,\sigma}^2 = m^2 + (2k + 1 - \sigma)|qB|\,. \tag{15}$$

The temperature dependence of $h_Q^B(m,T,B)$ can be seen in the right panel of Fig. 1. Here, the quark mass is fixed at 1 GeV and magnetic fields are 0 (the solid black line), 1.0 GeV^2 (the double-dot-dashed green line) and 2.5 GeV^2 (the dotted purple line). The external magnetic field increases the explicit center symmetry breaking strength and hence its role is opposite to the quark mass.

In this work, we apply the mean-field approximation in which the real and imaginary parts of the Polyakov loop are obtained by solving the gap equations

$$\frac{\partial \mathcal{U}}{\partial x} = \frac{\partial \mathcal{U}}{\partial y} = 0\,. \tag{16}$$

For a real and positive h, the expectation value of the imaginary part vanishes. Nevertheless, one can still explore fluctuations in both longitudinal (real) and transverse (imaginary) directions which are related to the inverse of the curvature matrix

$$T^3\chi_{\mathrm{L}} = \left(\mathcal{C}^{-1}\right)_{11}\,, \qquad T^3\chi_{\mathrm{T}} = \left(\mathcal{C}^{-1}\right)_{22}\,, \tag{17}$$

with

$$\mathcal{C} = \begin{pmatrix} \frac{\partial^2 \mathcal{U}}{\partial x^2} & \frac{\partial^2 \mathcal{U}}{\partial x \partial y} \\ \frac{\partial^2 \mathcal{U}}{\partial x \partial y} & \frac{\partial^2 \mathcal{U}}{\partial y^2} \end{pmatrix}\,, \tag{18}$$

which is evaluated at point (x_0, y_0) satisfying the gap equations (16). Longitudinal and transverse susceptibilities can be composed into the following ratio [11, 12]:

$$R_{\mathrm{T}} = \chi_{\mathrm{T}}/\chi_{\mathrm{L}}\,, \tag{19}$$

which has been found to be a robust probe of deconfinement by LQCD studies [11, 13]. Moreover, it is sensitive to Z_3 symmetry and spontaneous as well as the explicit breaking [14]. Another observable relevant for studying deconfinement is the static quark entropy

$$S_Q = \frac{\partial}{\partial T} T \ln\langle L\rangle \tag{20}$$

which was argued to provide a scheme-independent way of defining the critical temperature of deconfinement from tracking its peak [13].

3. Polyakov loop fluctuations for heavy quarks

Before the discussion of numerical results obtained within the current model, we examine the efficacy of the linear approximation of the full one-loop potential. To this end, we compared the Polyakov loop dependence of the full potential (with the subtracted $\mathcal{U}_0$ term) and the linear approximation for the single quark flavor. In the case of the heavy quark, $m_q = 0.8$ GeV,

(the left panel of Fig. 2) the full potential results (dots and triangles) and linear approximation (lines) are almost indistinguishable for both vanishing magnetic field (the solid black line) and finite qB (the dashed red line). The temperature is fixed at 0.2 GeV. Hence, the linear approximation provides an excellent description of the full potential for heavy quarks. Surprisingly, the linear approximation remains reliable even for massless quarks in the absence of magnetic field (see solid black line in the right panel of Fig. 2). However, this is no longer true for finite magnetic field. Especially, for massless quarks, the linear approximation is not reliable for fields relevant for studying chiral dynamics ($qB \sim 0.25\,\mathrm{GeV}^2$, see the dashed red line in the right panel of Fig. 2).

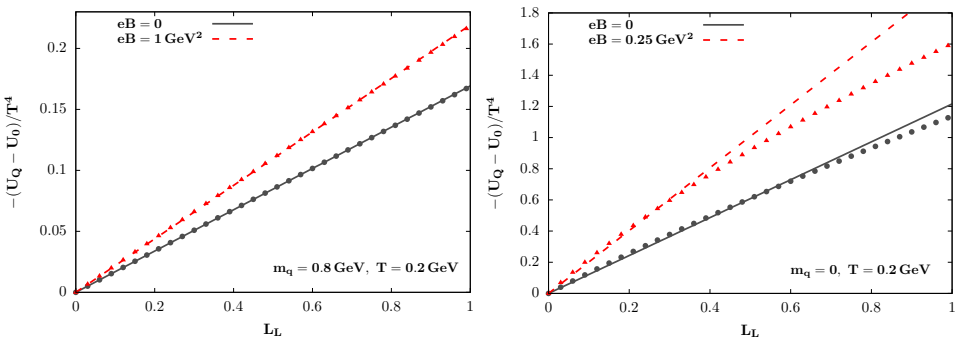

Fig. 2. (Color online) Comparison between the full quark potential (points) and its linear approximation (lines) for a heavy quark ($m_q = 0.8\,\mathrm{GeV}$, the left panel) and massless quark (the right panel). Solid black lines: vanishing magnetic field, dashed red lines: finite magnetic field.

We now describe results on the Polyakov loop and its fluctuations for the single-flavor heavy quarks. The first-order transitions are stable under small symmetry breaking [15] and hence, there exists a critical quark mass for which, in absence of other parameters, the deconfinement turns into the second-order transition. For the model used in the current study, the critical value is $m_0 = 1.1\,\mathrm{GeV}$ for one quark flavor. The left panel of Fig. 3 shows the temperature dependence of the real part of the Polyakov loop, calculated for quark mass $1.4m_0 = 1.54\,\mathrm{GeV}$. Since the quark mass is above the critical value, the deconfinement for the vanishing magnetic field is first-order and the Polyakov loop is discontinuous (the solid red line). The external magnetic field enhances the breaking of the center symmetry and for its sufficiently large value ($qB = 3m_0^2$, the dash-dotted green line), the deconfinement reaches the critical point and, for even larger values of qB, it becomes a crossover (the dashed blue). The right panel of Fig. 3 shows the static

quark entropy. It is discontinuous for the first-order transition, diverges at the critical point and has a finite peak at crossover which makes it a robust probe of deconfinement.

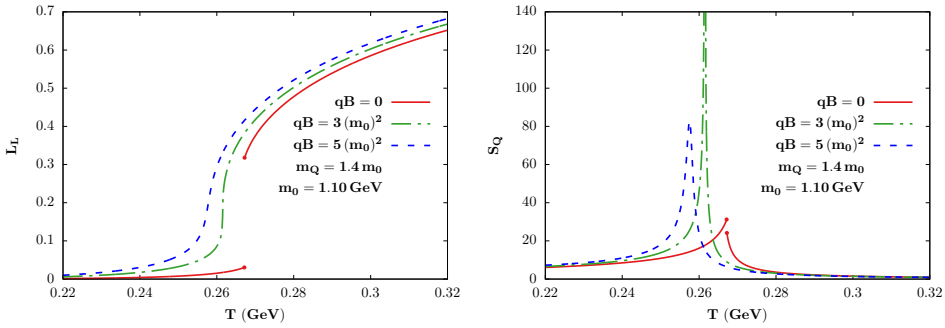

Fig. 3. (Color online) The Polyakov loop expectation value (the left panel) and static quark entropy (the right panel) for the fixed quark mass, $m_q = 1.4m_0$, and different values of the magnetic field.

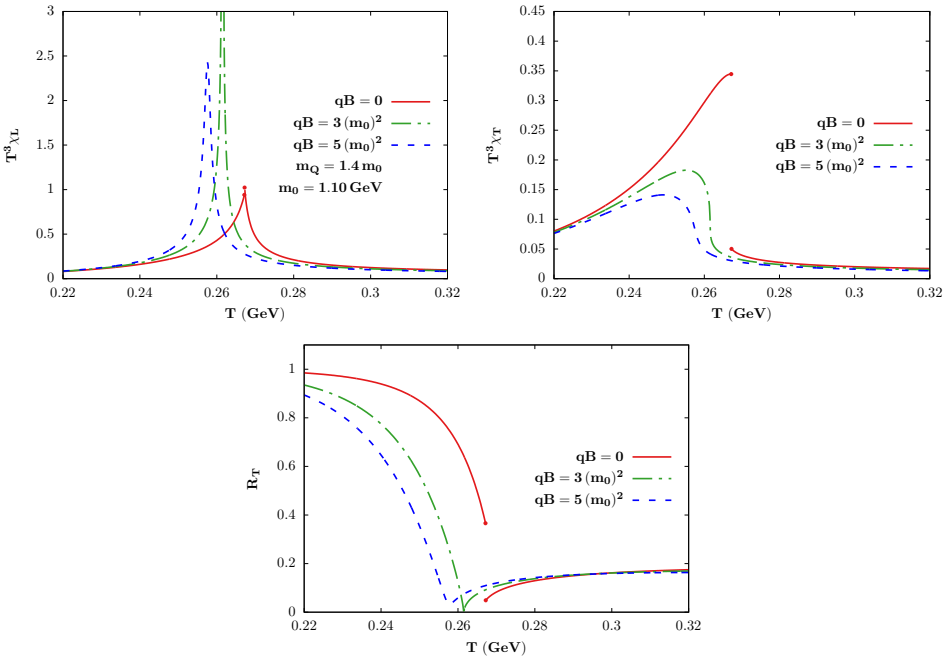

Fig. 4. (Color online) The longitudinal (the upper left panel) and transverse (the upper right panel) Polyakov loop susceptibilities as well as their ratio R_T (the lower panel) for the fixed quark mass, $m_q = 1.4m_0$, and different values of the magnetic field.

Corresponding susceptibilities can be seen in Fig. 4, where the upper left panel corresponds to the longitudinal susceptibility and the upper right panel to the transverse one, respectively. The longitudinal susceptibility is discontinuous at the first-order transition, diverges at the deconfinement critical point and has a finite peak in the crossover region. While the transverse susceptibility is also discontinuous for the first-order transition, it does not diverge at the critical point, in comparison to the longitudinal one. The lower panel shows the corresponding R_{T} ratio. At low temperature, R_{T} is close to one (the limit following from the Z_3 symmetry [11]) and it decreases rapidly with the temperature in the transition region.

4. Deconfinement temperature in case of light quarks

The model described in this work may be useful for understanding why the naive implementation of the PNJL model leads to increasing deconfinement temperature. The explicit center symmetry breaking increases with

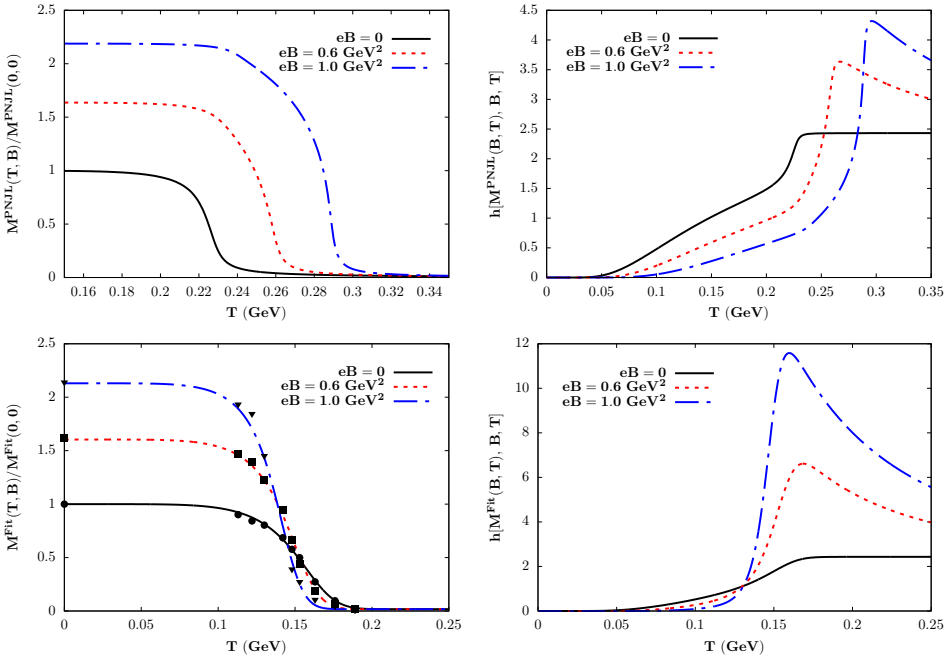

Fig. 5. (Color online) The upper left panel: quark mass profiles obtained with the PNJL model for three values of the magnetic field. The upper right panel: the corresponding effective Z_3 breaking strength. The lower left panel: quark mass profiles obtained with the LQCD data on the quark condensate for three values of the magnetic field. The lower right panel: the corresponding effective Z_3 breaking strength.

the magnetic field and decreases with the quark mass. For a PNJL model, one can introduce an effective Z_3 breaking strength, $h[M(T,B),T,B]$, which becomes a function of the dressed quark mass $M(T,B)$. An illustrative calculation of the constituent quark mass can be seen in the upper left panel of Fig. 5 (the details of calculations can be found in Ref. [4]). At low temperatures, quark mass increases with the magnetic field which is a manifestation of the magnetic catalysis (which can be captured by most of NJL models). The increase of quark mass is sufficient to overcome the enhancing effect on h due to magnetic field in the temperature range relevant for the crossover (see the upper right panel of Fig. 5) and, in consequence, the deconfinement temperature increases (see the dashed red curve in Fig. 6).

The lower left panel of Fig. 5 shows the LQCD-improved quark mass profile (see Ref. [4] for details). Points are obtained using the lattice data from Ref. [16]. The lower right panel shows the corresponding center symmetry breaking strength which is strongly enhanced by the magnetic field and leads to decreasing deconfinement temperature (see the solid black curve in Fig. 6). Therefore, the competing effects of the quark mass and magnetic field lead to opposite trends of the magnetic field dependence of deconfinement temperatures in case of LQCD and PNJL model.

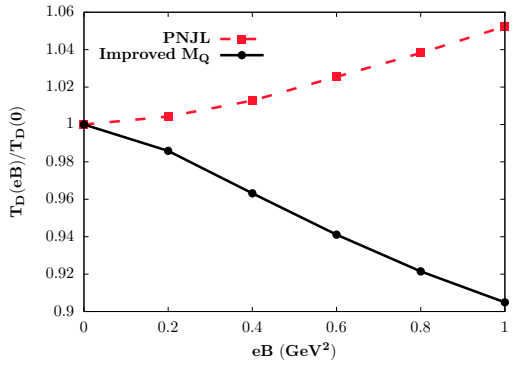

Fig. 6. (Color online) Deconfinement temperature as a function of magnetic field for the PNJL model (upper curve) and the improved quark mass profile (lower curve).

5. Conclusions

In this work, we discussed the impact of a finite magnetic field on the explicit center symmetry breaking strength and deconfinement of heavy quarks. We found that $h(T,B,m)$ increases with the magnetic field. Consequently, deconfinement phase transition is shifted towards lower temperatures which was shown by studying the Polyakov loop and its susceptibili-

ties in the heavy-quark regime within an effective model. Especially, for the sufficiently strong magnetic field, the first-order transition turns into the crossover. Additionally, we calculated the ratio of susceptibilities and static quark entropy which are also sensitive probes of deconfinement.

With the model described in this work, we also demonstrated a subtle interplay between chiral dynamics and deconfinement using quark mass profiles obtained from the PNJL model and lattice-inspired parametrization. This example may be useful for developing more accurate effective models of QCD.

The author acknowledges helpful comments and fruitful discussions with Pok Man Lo, Michał Marczenko, Krzysztof Redlich and Chihiro Sasaki. This work was partly supported by the National Science Centre, Poland (NCN), under OPUS grant No. 2018/31/B/ST2/01663.

REFERENCES

[1] J.O. Andersen, W.R. Naylor, A. Tranberg, *Rev. Mod. Phys.* **88**, 025001 (2016).

[2] F. Bruckmann, G. Endrődi, T.G. Kovács, *J. High Energy Phys.* **1304**, 112 (2013).

[3] M. D'Elia, F. Manigrasso, F. Negro, F. Sanfilippo, *Phys. Rev. D* **98**, 054509 (2018).

[4] P.M. Lo, M. Szymański, C. Sasaki, K. Redlich, *Phys. Rev. D* **102**, 034024 (2020).

[5] J. Greensite, *Prog. Part. Nucl. Phys.* **51**, 1 (2003).

[6] E.S. Swanson, *AIP Conf. Proc.* **717**, 36 (2004).

[7] A.M. Polyakov, *Phys. Lett. B* **72**, 477 (1978).

[8] G. 't Hooft, *Nucl. Phys. B* **38**, 1 (1978).

[9] B. Svetitsky, L.G. Yaffe, *Nucl. Phys. B* **210**, 423 (1982).

[10] K. Fukushima, V. Skokov, *Prog. Part. Nucl. Phys.* **96**, 154 (2017).

[11] P.M. Lo *et al.*, *Phys. Rev. D* **88**, 014506 (2013).

[12] P.M. Lo *et al.*, *Phys. Rev. D* **88**, 074502 (2013).

[13] A. Bazavov *et al.*, *Phys. Rev. D* **93**, 114502 (2016).

[14] P.M. Lo, M. Szymański, K. Redlich, C. Sasaki, *Phys. Rev. D* **97**, 114006 (2018).

[15] K. Binder, *Rep. Prog. Phys.* **50**, 783 (1987).

[16] G.S. Bali *et al.*, *Phys. Rev. D* **86**, 071502 (2012).